Indonesian Journal of Science & Technology 7(1) (2022) 117-130

Indonesian Journal of Science & Technology

Journal homepage: http://ejournal.upi.edu/index.php/ijost/

Crosslinked Spin-Assisted Layer-by-Layer Polyelectrolyte Nanofiltration Membrane: From Literature Review to Experiment

Farid Fadhillah [1,*]

[1]Chemical Engineering Department, Imam Mohammad Ibn Saud Islamic University, Saudi Arabia
Correspondence: E-mail: fffadhillah@imamu.edu.sa/faridfad.imamu@gmail.com

ABSTRACT

Layer-by-Layer (LbL) assembly is considered as the most versatile and robust method in thin-film fabrication. However, its use in the preparation of desalination membrane is still in its infancy. Spin-assisted layer-by-layer assembly (SA-LbL), one of the LbL variants, was selected for the fabrication of a nanofiltration membrane due to its versatility to produce an ultra-thin film with highly controlled film properties within an incredibly short time. Branched-polyethyleneimine (PEI) and poly(sodium 4-styrenesulfonate) (PSS) were employed and alternately deposited on the top of the ultrafiltration polyethersulfone (PES) substrate. PEI/PSS film was then crosslinked using Gluteraldehyd (GA). The resulting membrane was tested at a feed concentration of 2000 ppm NaCl, a pressure of 10 bar, and a temperature of 25°C. Crosslinking time and many layers were varied to investigate the extent of crosslinking and its impact on membrane performance. The permeation test of $(PEI/PSS)_{10}$ crosslinked for 6 hours showed rejection of 94.2 % and water flux of 4.2 $L/h\cdot m^2$ meanwhile uncrosslinked $(PEI/PSS)_{35}$ showed rejection of 75.66% only. The result showed that crosslinking improved the rejection of NaCl with a smaller number of layers. This result also displayed SA-LbL method is promising and can be used to produce membrane suitable for NF or RO application.

ARTICLE INFO

Article History:
Submitted/Received 09 Dec 2021
First revised 16 Jan 2022
Accepted 01 Mar 2022
First available online 04 Mar 2022
Publication date 01 Apr 2022

Keyword:
Desalination,
Layer by layer,
Nanofiltration,
Polyelectrolyte,
Reverse osmosis,
Spin coating.

Abbreviation

PEI : polyethylene imine
PSS : poly(sodium 4-styrenesulfonate)
PDAC : polydiallyldimethylammonium chloride
PAN : polyacrylonitrile
PVAm : polyvinyl amine
PVS : polyvinyl sulfate
PAH : polyallylamine hydrochloride
GA : glutaraldehyde
PSF : polysulfone
PES : polyethersulfone
SDS : sodium dodecyl sulfate

1. INTRODUCTION

The availability and accessibility to freshwater are one of the most pervasive problems that humanity is facing nowadays and near future. Water desalination, water reuse, and water decontamination are considered the main solution for addressing the problem with freshwater (Shannon *et al.*, 2008). The membrane has been widely known as the only technology at the moment that can execute all the above solutions. Several membrane types can be used for this purpose such as nanofiltration, reverse osmosis, and forward osmosis membranes.

Nanofiltration becomes more and more popular owing to its ability to remove small contaminants in the range of 100-5000 Da MWCO such as small protein, multivalent salts, etc. (Touir *et al.*, 2021) while still producing relatively high-water flux. Hence, NF has made membrane separation becomes more competitive in terms of selectivity and cost since the establishment of a thin-film composite membrane in the 1980s (Oatley-Radcliffe *et al.*, 2017). The popularity is shown by the increasing trend of the research paper published in the field of nanofiltration as portrayed in **Figure 1**. There is a sharp decline in 2022 which is most likely due to the covid-19 pandemic. Indeed, this hinders many research activities in various fields (Razon, 2020).

NF membrane has been widely used in various applications such as the removal of heavy metals (Li *et al.*, 2022), water hardness (Hu *et al.*, 2022), dye (Ahmadipouya *et al.*, 2022; Lau *et al.*, 2009), organic micropollutant (Yacouba *et al.*, 2021), virus (Barro *et al.*, 2021), etc. Even though, its low resistance to biofouling is still most problematic until now. It is a common problem found in various membrane applications as well. This problem stems from membrane material i.e., polyamide, and its fabrication method i.e., interfacial polymerization. As widely known that polyamide is used in commercial RO or NF membranes since the era of NS100 or FT-30 polyamide composite membrane. Unfortunately, there has been no major improvement in this type of membrane material from a chemistry point of view (Petersen, 1993). Polyamide is generally known for its hydrophobicity meanwhile the fabrication method that is interfacial polymerization (IP) lacks fine-tuning ability to control surface properties such as roughness, hydrophilicity, composition, etc. All these reasons result in polyamide membranes suffering from the above problem.

Thus, research effort in the last couple of decades in this field has mainly been directed to the development of novel membrane materials to combat fouling problems. The development includes the use of inorganic membrane materials, the incorporation of nanoparticles, and the utilization of polymers having high hydrophilicity and versatile processability to produce smooth and thin layers (Lee *et al.*, 2011).

Layer-by-layer (LbL) assembly is regarded as the most versatile and robust technique that can embrace many requirements to fabricate an excellent NF or RO membrane. It is a thin film fabrication technique that can provide a conformal LbL coating of a variety of functional materials on various substrates (Decher, 1996). The LbL coating is simply done by immersing the substrate alternately into a polycation and polyanion until the desired number of layers is attained. Although the technique is simple, it offers incredible flexibility in controlling the properties of the deposited layer including thickness, composition, smoothness, charges, etc. Therefore, the use of dip-LbL or sometimes called immersive LbL, for preparing NF membrane has attracted attention from researchers as shown by the increasing number of research publications every year as illustrated in **Figure 2**. A more detailed literature review on this field can be found in section 2 of this paper.

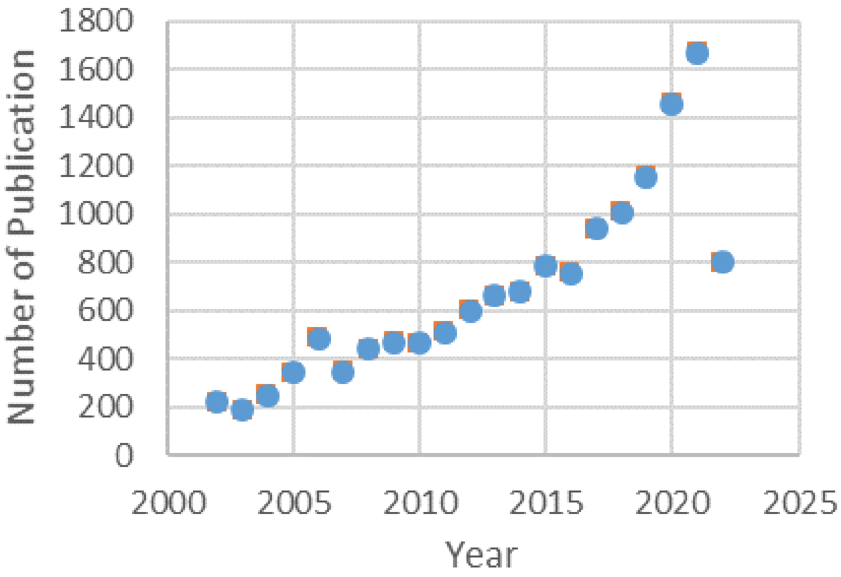

Figure 1. Number of the research paper published in the field of Nanofiltration for the last 20 years (2002-2022) (based on data from sciencedirect.com).

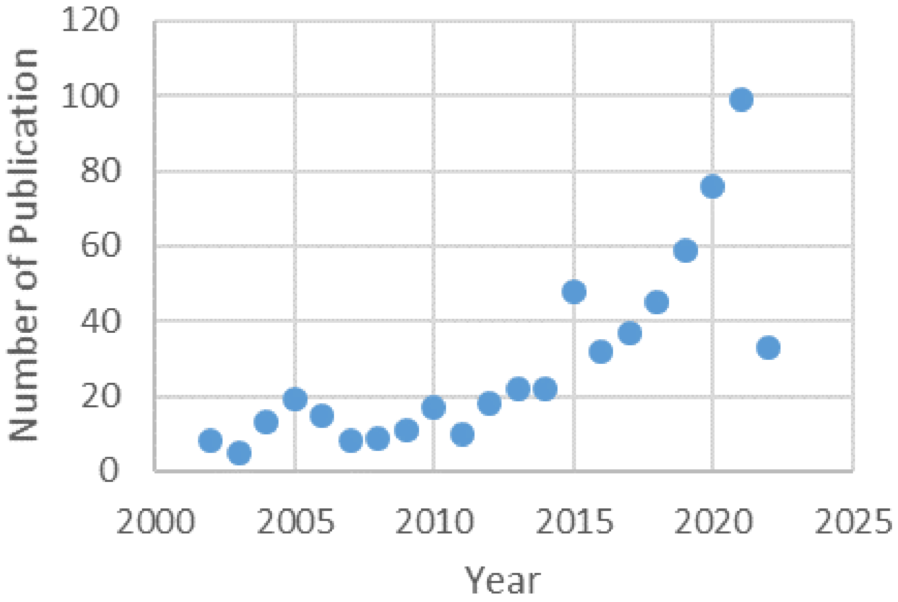

Figure 2. Number of the research paper published in the field of polyelectrolyte multilayer nanofiltration for the last 20 years (2002-2022) (based on data from sciencedirect.com).

2. LITERATURE REVIEW

Layer-by-layer assembly is rediscovered by Decher (Decher & Schmitt., 1992; Schmitt *et al.*, 1993) and the method is established a few years later (Decher, 1996). At the beginning of its development, an ultrathin film is prepared through alternate deposition of the layer of anionic and cationic polyelectrolytes on a support or substrate. The method utilizes the electrostatic force between oppositely charged polyelectrolytes. A complete cycle consisting of anionic and cationic polyelectrolytes can be repeated until the desired number of cycles is attained (Decher, 1996). Nowadays, LbL is not only using electrostatic force to produce the thin film but also via various molecular interactions such as hydrogen bond (Wang *et al.*, 2018), covalent bond (Zhang *et al.*, 2021), and dipolar interaction (Qiao *et al.*, 2008). Therefore, LbL can be used as far as there is molecular interaction between molecules of deposited materials. This feature makes LbL assembly a truly robust and versatile thin film fabrication technique.

In the classical LbL assembly, polyelectrolytes are adsorbed naturally on the substrate. It is generally known that adsorption is a slow process thus the overall dip LbL assembly is a time-consuming process, which can use up to 15 min to deposit only a single layer of polyelectrolyte (Richardson, 2015). Two variants of LbL are then invented i.e., spray LbL and spin-assisted LbL with the main purpose of reducing the deposition time. Spray LbL is invented in 2000 (Schlenoff *et al.*, 2000) while spin-assisted LbL is invented a year after (Chiarelli *et al.*, 2001; Cho *et al.*, 2001).

In SA-LbL, anionic and cationic polyelectrolytes are alternately cast on to the spinning substrate or ontothe substrate and spun afterward. Due to high-speed spinning i.e., 3000 rpm in our work, the adsorption occurs extremely fast. It is because polyelectrolyte chains rearrangement and water removal occur simultaneously within a very short time. Quick water removal promotes faster adsorption and stronger electrostatic force thus more polymer chains are adsorbed within a short time.

Briefly, the adsorption step which is considered the limiting step in the dip-LbL assembly has been improved tremendously in the case of SA-LbL. Air shear force that occurs due to the relative movement between the spinning substrate and air enhances the planarization of multilayer film and significantly reduces the surface roughness of the film (Chiarelli *et al.*, 2001; Cho *et al.*, 2001).

Although dip-LbL is a slow process, it is still the standard procedure and the most used method for preparing PEM NF membrane. There are various applications of PEM LbL NF membrane have been reported but only some representative and notable works are presented in **Table 1**, particularly those that are comparable to our work.

The first work using dip LbL for NF application was reported by Krasemann and Tieke in 2000. It was for the first time; this type of membrane can be used as an NF membrane. However, this work did not mention the rejection of specific salt but rather reported the selectivity between Mg^{2+} and Na^{+}, which was up to 112.5 using $(PAH/PSS)_{60}$ membrane. The time required for preparing the membrane is, unacceptable, very long, up to 120 hours to fabricate one $(PAH/PSS)_{60}$ NF membrane (Krasemann *et al.*, 2000).

Jin *et al.* (2003) reported PEM membrane to consist of $(PVAm/PVS)_{60}$ for NF and RO application. The result was quite promising by showing complete rejection for Mg^{2+} while displaying 84% NaCl rejection (Jin *et al.*, 2003). It was a fair performance, but they evaluated the membrane at low salt concentration, i.e., 584 ppm. The membrane performance may deteriorate when tested at much higher salt concentrations. Another deficiency in this work was the very long preparation time and relatively low flux.

Table 1. Layer-by-Layer membrane performance comparison.

Membrane	Method	Testing condition	Result (Rejection; Permeability)	Ref
$(PVAm/PVS)_{60}$	Dip LbL on PAN/PET	584 ppm NaCl; 25°C; 5 bar	84%; 0.2 L/h·m^2·bar	(Jin *et al.*, 2003)
$(SA/CHI)_{25}$	Dip LbL	1985.6 ppm NaCl; 25°C; 16 bar	75%; 1.2 L/h·m^2·bar	(Lajimi *et al.*, 2004)
$(SA/CHI)_{25}$	Dip LbL on Electrospun CA fiber	2000 ppm NaCl; 25°C; Vacuum Pressure	14%; flux: 40 L/h·m^2	(Ritcharoen *et al.*, 2008)
$(PAH/PSS)_3$	Dip-LbL on hollow fiber PES UF	1000 ppm $MgCl_2$; 25°C; 2 bar	96%; 6 L/h·m^2·bar	(Rajabzadeh *et al.*, 2014)
$(PAH/PSS)_{10}$	Spray LbL Crosslinked on PSF	NaCl: 2000 ppm T: 25°C; P: 24 bar	90%; 0.33 L/h·m^2·bar	(Cho *et al.*, 2015)
(PEI/PAA) $[MPD/TMC]_{15}$	Molecular-dip LbL	2000 ppm NaCl T: 25°C; P: 15.5 bar	98.7% ;1.34 L/h·m^2·bar	(Gu *et al.*, 2015)
$(PDAC/PSS)_{20}$	Dip-LbL on hollow fiber PES UF	292 ppm NaCl, 25°C; 2 bar	46%; 7 L/h·m^2·bar	(Kamp *et al.*, 2021)
$(PDAC/SDS/PSS)_5$	Dip-LbL on PAN UF	1000 ppm NaCl, 25°C; 4 bar	30%; 11.5 L/h·m^2·bar	(Liang *et al.*, 2021)
$(PEI/PSS)_{10}$	Crosslinked-SA-LbL on PES UF	2000 ppm NaCl; 25°C; 10 bar	94.2%; 0.42 L/h·m^2·bar	This work

The use of other LbL variants such as spray LbL was first time reported by Cho *et al.* using crosslinked $(PAH/PSS)_{10}$, their membrane showed NaCl rejection of 90%, flux of 0.33 L/h·m^2·bar while achieving $MgCl_2$ rejection of around 95%. It showed much better rejection and flux compared to those of dip LbL. Their work also showed that the membrane has high chlorine resistant (Cho *et al.*, 2015).

Dip-LbL was also utilized to fabricate polyamide membrane, which is usually prepared through conventional IP. The method is called molecular layer-by-layer according to the author. Although their membrane showed improved rejection and flux, the membrane itself seems similar to a typical TFC polyamide membrane, except for the presence of an interlayer made of PEI/PAA between the polyamide layer and support layer. The deposition of MPD and TMC was also done following the dip-LbL method. Unfortunately, the surface properties of their membrane were not reported in detail. Whereas SEM images in their work suggest the surface properties are similar to that of a typical polyamide membrane. In other words, this method may not solve the problem with the existing polyamide membrane.

Based on the above literature review, we proposed the use of spin LbL assembly to fabricate the PEM membrane. For the first time, the NF SA LbL membrane was fabricated by employing PDAC/PSS. The membrane showed an $MgCl_2$ rejection of 94.6% and a flux of 3.32 L/m^2·h tested at 2000 ppm $MgCl_2$ (Fadhillah *et al.*, 2020).

Even though the performanwas promising, the rejection dropped as $MgCl_2$ concentration in the feed stream was further increased. It suggests the membrane's significant swelling when exposed to water with higher salinity (Dubas & Schlenoff., 2001). It is also expected that its performance degrades when exposed to NaCl solution. For the above reason, we then employed branched-PEI/PSS instead, because of the possibility to crosslink PEI using GA. PEI is a weak polyelectrolyte whose degree of ionization is a strong function of pH (Yoo *et al*., 2010) meanwhile PSS is a strong polyelectrolyte whose degree of ionization remains constant at any pH (Wu *et al*., 2017). Meanwhile, Glutaraldehyde (GA) was used as a chemical crosslinker.

In summary, it is the first time for PEI/PSS NF membrane to be prepared using SA-LbL. This work is essentially a complementary study on the utilization of such technique to fabricate NF or RO membrane. The work eventually provides a better understanding of SA-LbL membrane characteristics and behavior. For the interested reader, a preliminary study on the fabrication of this membrane using SA-LbL has already been reported recently by our research group members (Alghamdi, 2021). His work includes the study of the effect of the number of layers and pH on membrane performance while in our work, we elaborate more study on crosslinking effect on membrane performance.

3. METHODS

3.1. Materials

Branched-polyethyleneimine (B-PEI) with a molecular weight of 25,000 by LS and poly(sodium 4-styrenesulfonate) (PSS) with a molecular weight of 70,000 in the form of a 30 wt% in H_2O solution were purchased from Sigma-Aldrich (USA). Technical grade glutaraldehyde 5.6 M, 50% in H_2O was also purchased from Sigma-Aldrich. Extra-pure NaCl was obtained from Pharmchem (India). All the polyelectrolytes were used without further purification. PES ultrafiltration (UF) membranes (YMPWSP3001, Sterlitech Corp., USA) with a pore size corresponding to a molecular weight cut-off of 10 kDa were used as the support layers. The molecular structure of the main materials is shown in **Figure 3**. All solutions were prepared using ASTM type 1 water (18.2 MΩ, 0.055 mS/cm).

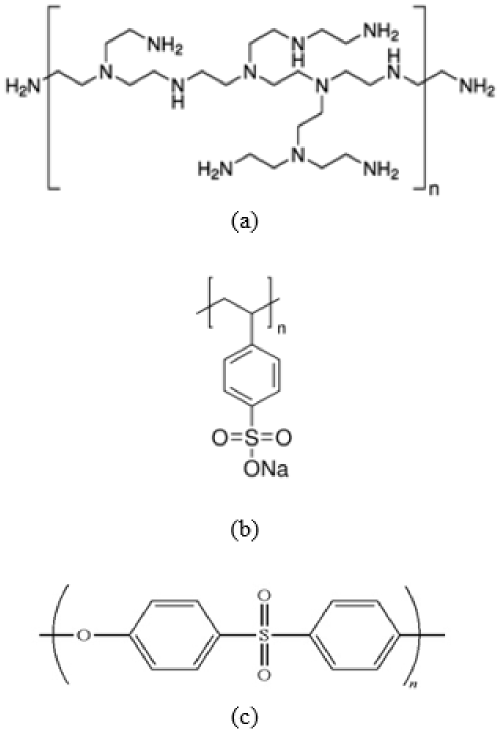

Figure 3. Molecular structures of materials used to synthesize PEM TFC membranes: (a) Branched PEI (b)PSS, and (c) PES.

3.2 Polyelectrolyte Membrane (PEM) Thin Film Composite (TFC) Fabrication

PES UF membrane was used as a support layer and was pretreated in a plasma cleaner (PDC-32-G-2, Harrick Plasma Inc) following a procedure described elsewhere (Kim *et al.*, 2002). The pretreatment of PES is needed to clean the support surface before deposition and to introduce oxygen-containing polar groups, which make the surface more hydrophilic and highly negatively charge. PEI and PSS solutions with a concentration of 0.02 M were prepared with NaCl added to them until the concentration of NaCl in the solution reached 0.05 M. Finally, the pH of PEI and PSS solution was adjusted to pH 8 (Alghamdi, 2021).

The alternate deposition of PEI and PSS on PES was done as follows, firstly, the PEI solution was deposited on a spinning PES support at a rate of 0.2 mL/s for 10 s, and the resulting film was subsequently spin-dried for 20 s. The PES support was spun at a speed of 3000 rpm (Fadhillah *et al*., 2011). The dry film was then rinsed with deionized (DI) water at a rate of 0.8 mL/s for 10 s to remove any weakly bonded polyelectrolyte molecules. This was then followed by another spin-drying for 14 s. The PSS solution was deposited exactly in the same way as the PEI solution was. After this deposition, the cycle is completed and can be repeated as many as required.

After completion of the deposition, the resulting polyelectrolyte multilayer (PEM) membrane was then rinsed thoroughly before crosslinking step. Glutaraldehyde (GA) with a concentration of 3 M was prepared and PEM was immersed in GA solution within the desired time to study the effect of crosslinking time between PEM and GA on the membrane performance. After crosslinking process was finished, the PEM membrane was rinsed and stored in distilled water overnight before the permeation test. The schematic diagram of membrane fabrication is presented in **Figure 4**.

3.3 Characterization

3.3.1 Film thickness

SA-LbL film thickness measurement was done using a KLA Tencor AlphaStep® D-500 stylus profilometer. A stylus speed of 0.05 mm/s with a stylus force of 0.2 mg was employed during the measurement. The thickness measurement was taken at 4 different locations on each sample.

3.3.2 Hydrophilicity

Membrane hydrophilicity was done using Biolin Theta Flex® optical tensiometer. A 10 μL water droplet at 20°C was dispensed on the membrane surface while a live-contact angle analysis of the water drop on the membrane surface was done for 10 seconds

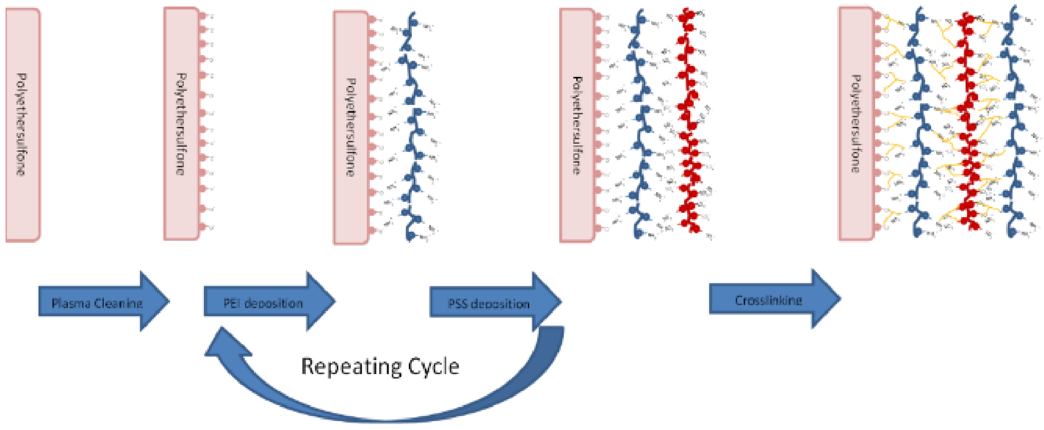

Figure 4. Membrane preparation method.

3.3.3 Surface charge

Surface charge is another important membrane property. For this purpose, Anton Parr Surpass 3$^{(R)}$ surface zeta potential analyzer was utilized. The measurement was done using 0.01 M KCl solution at the temperature of 24 ± 1.43°C and pH of 5.48 ± 0.08 meanwhile the interfacial double layer above the membrane surface during the potential measurement was maintained exactly at 100 μm.

3.4 Permeation Test

Permeation tests were performed for 5 h after the membrane was kept overnight for equilibration under wet conditions. The test was done using a crossflow permeation cell (Innovator® CF016, Sterlitech Corporation), having an active membrane surface area of 20.6 cm^2. The conditions for the permeation tests were as follows: the pressure of 10 bar, feed temperature of 25.44 ± 1.02°C, cross-flow velocity (CFV) of 0.65 m/s, and NaCl concentration of 2000 ppm. Meanwhile, the pH of the feed solution remained stable at approximately 6.6 without requiring any adjustments.

4. RESULTS AND DISCUSSION

PEM membrane consisting of PEI/PSS bilayers was successfully fabricated using SA-LbL assembly on PES UF membrane support. The membrane showed promising results with comparable performance or even better to other works as seen in **Table 1**. Our previous work (Alghamdi & Fadhillah, 2020) showed that at higher salinity, the rate of rejection decreased mainly due to membrane swelling (Dubas & Schlenoff., 2001). Therefore, in this work, the membrane was crosslinked employing glutaraldehyde to improve PEM stability when it was being exposed to high salinity water (Dubas & Schlenoff., 2001). During the crosslinking, the amino group carried by PEI forms an ionic bond with the carbonyl group carried by GA as described elsewhere (Wang *et al*., 2020). In this work, the effect of crosslinking time on various PEI/PSS membranes was investigated concerning membrane performance i.e., rejection and permeability.

The successful coating of PEI/PSS layers on PES support was shown by the thickness build-up as illustrated in **Figure 5**. PEI/PSS layers were crosslinked for an hour and stored in distilled water overnight before measurement. As shown, PEI/PSS grew linearly starting from around 10 layers of deposition. It implies that the effect of the substrate has been diminished.

One can also see that the film is quite thick, for instance, about 385 nm thick layer was attained within 35 layers of PEI/PSS. This is because the presence of 0.05 M NaCl in polyelectrolyte solution results in coiled polyelectrolyte chain conformation. In addition to that, fast polyelectrolyte adsorption during spinning enhances a higher amount of adsorbed polyelectrolyte on PES support.

Table 2 shows the variation of film characteristics i.e., surface charge and hydrophilicity. The change was not only because of the increase in the number of layers but also because of crosslinking. As shown, pristine PEI support was relatively hydrophobic shown by a higher degree of contact angle. The membrane became more hydrophilic when it was coated with PEI/PSS indicated by the increase in contact angle. It is important to note that plasma treatment prior to polyelectrolyte deposition introduces an oxygen-containing polar group, which makes the support extremely hydrophilic. The highly hydrophilic nature remained intact even after the deposition few layers indicating the effect of support was still operative. However, its effect gradually decreased until around ten layers. This result is also consistent with thickness measurement.

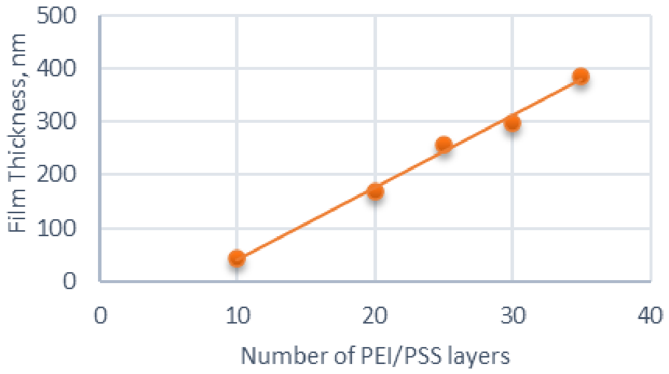

Figure 5. Crosslinked PEI/PSS film thickness growth.

Table 2. Contact angle and Membrane surface charge of uncrosslinked and crosslinked PEI/PSS layers.

Number of (PEI/PSS) Layer	Contact angle, °		Surface Charge, mV	
	Uncrosslinked	**Crosslinked**	**Uncrosslinked**	**Crosslinked**
0 (PES support)	64.35 ± 0.83	64.35 ± 0.83	-19.89	-19.89
2	8.02 ± 0.05	-	-2.86	-
4	12.88 ± 0.13	-	1.2	-
6	18.73 ± 0.67	-	6.62	-
8	32.26 ± 0.07	-	10.66	-
10	32.10 ± 0.24	32.74 ± 1.56	18.25	-18.20
20	34.97 ± 0.11	36.06 ± 1.30	21.94	-21.91
30	36.96 ± 0.04	38.28 ± 0.10	33.49	-17.33
35	38.60 ± 0.06	-	33.42	-

It can also be seen in **Table 2** that uncrosslinked film was positively charged although the outermost layer was PSS, a negatively charged polyelectrolyte. This result indicates the overall film properties are not determined by the outermost layers but rather by charge overcompensation between branched PEI and PSS. Positively charged functional groups of PEI were partially compensated by negatively charged functional groups of PSS resulting in the overall film being positively charged. When the film was crosslinked, it became negatively charged regardless deposited number of layers. The result also suggested that the uncompensated amine group of PEI has been successfully crosslinked with the carbonyl group of GA. Hence, the surface charge of the overall film is now determined by the outermost layer, which is PSS in this case and shows negatively charged instead.

4.1. Crosslinking Time

Understanding the crosslinking mechanism in a nonporous film is important to determine, in which step is considered as the limiting step. This is required to find the most optimum crosslinking time. A complete study on this topic needs process modeling and simulation including all possible steps, which are beyond the scope of this reported work. Nevertheless, this work is intended to show the extent of crosslinking qualitatively by analyzing the membrane performance affected by crosslinking.

In this work, GA with a concentration of 3 M was prepared. PEM that was just prepared and thoroughly rinsed was immediately soaked in glutaraldehyde solution at the desired time.

Diffusion is a slow process and time is needed for GA to diffuse further inside the PEM. A higher amount of GA in the PEM film enhances reaction with the uncompensated amine group of PEI. GA here acts as a bridge connecting between PEI layers. The crosslinking produced a more entangled and compact film keeping the PEM from excessive swelling during contact with saline water.

Along with the above result, one can also notice a fast increase in the rejection (see **Figure 6(a)** dan **(b)**) occurred at the beginning after the PEM immersion in GA solution. In this case, the rejection increased from 75.66% for uncrosslinked $(PEI/PSS)_{35}$ to 89.2% within 1-hour crosslinking.

This observation indicated fast GA dissolution and diffusion through outer layers and immediately followed by the crosslinking reaction. As time proceeded, the outer crosslinked layers became a barrier for GA to diffuse in subsequent layers thus the crosslinking process was hampered. Therefore, it showed only a slight rejection increase when the time was even doubled up from 1 to 3 hours or 6 hours.

4.2. Effect of Crosslinking on PEM with different number of layers.

In the previous section, one can observe the relation between the crosslinking time and membrane performance. In this section, the crosslinking time is fixed whereas the number of layers is varied.

Figure 7 depicts the effect of crosslinking in PEI/PSS film at the one-hour crosslinking time. As shown, the permeability (rectangular symbol) decreased quite significantly. The decrease in permeability is generally believed because it is inversely proportional to the membrane thickness. When the number of layers was increased, the membrane thickness was also increased as shown in thickness build-up in **Figure 5**.

Meanwhile, the rejection (circle symbol) was almost constant at around 87% because it is not affected by membrane thickness. Rejection in the nanofiltration membrane is dictated by Donnan's exclusion and steric hindrance effect. The data presented in **Table 2** shows rather unvarying surface zeta potential after crosslinking regardless of the number of layers, which means rejection because the Donnan potential effect is similar for all PEM regardless of the number of layers. Whereas rejection due to steric hindrance effect is determined by the pore size of the PEM.

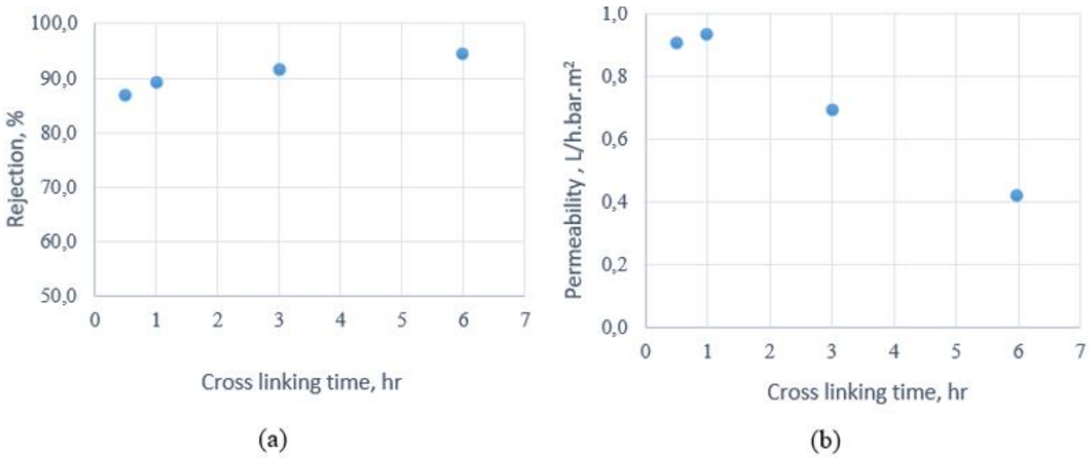

Figure 6. Effect of crosslinking time on the performance of PEM consists of (PEI/PSS)10 (a) rejection, (b) permeability. (Testing condition: P = 10 bar, T = 25.44 ± 1.02 C, CFV = 0.65 m/s, NaCl concentration = 1822 ± 127.43 ppm, and pH = 6.61 ± 0.38).

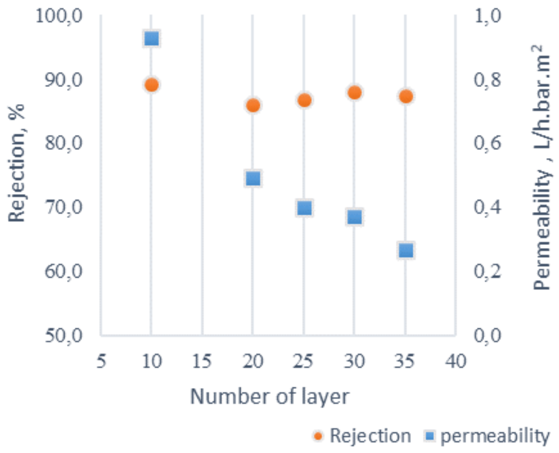

Figure 7. Effect of crosslinking on the performance of PEM consists of various PEI/PSS layers for crosslinking time of 1 h ((Testing condition: P = 10 bar, T = 25.44 ± 1.02°C, CFV = 0.65 m/s, NaCl concentration = 1822 ± 127.43 ppm, and pH = 6.61 ± 0.38).

The crosslinking of PEM is started from the outermost layer to deeper layers as GA kept on diffusing further inside the PEM until the prescribed time was attained. Because the crosslinking time was the same for all samples, the depth of crosslinked region in PEM was also practically similar for all samples. Consequently, it produced an almost similar pore size for all crosslinked PE. Therefore, both Donnan potential and steric hindrance did not vary significantly for all samples and produced similar rejection.

5. CONCLUSION

In this study, PEM TFC membranes consisting of crosslinked PEI/PSS were successfully fabricated employing SA-LbL assembly followed by chemical crosslinking with GA. The result showed that crosslinking improved the rejection of NaCl, and even higher rejection was attained with a much smaller number of layers i.e., rejection of around 90% for 10 bilayers only. It is a significant reduction in the number of layers, while the membrane still performed well enough (see **Table 1** for comparison).

Some works are still required to obtain complete knowledge about the membrane. The room for improvement is still widely open. For instance, testing PEI/PSS membrane in the harsher and more challenging environment including the presence of foulant and higher salinity; determining limiting steps in the crosslinking process to find the optimum crosslinking time; mixing with nanoparticles to improve fouling resistance, etc. Thus, participation from researchers all over the world is urgently required.

6. ACKNOWLEDGMENT

This work was funded by King Abdulazis City for Science and Technology (KACST) - National Science, Technology and Innovation Plan (NSTIP) under project number: 14-WAT68-08-R. I also acknowledge Dr. Ahmad M. Alghamdi from the chemical engineering department, Imam Mohammad Ibn Saud Islamic University for valuable his support and discussion.

7. AUTHORS’ NOTE

The authors declare that there is no conflict of interest regarding the publication of this article. The authors confirmed that the paper was free of plagiarism.

8. REFERENCES

Ahmadipouya, S., Mousavi, S. A., Shokrgozar, A., and Mousavi, D. V. (2022). Improving dye removal and antifouling performance of polysulfone nanofiltration membranes by incorporation of uio-66 metal-organic framework. *Journal of Environmental Chemical Engineering*, 10(3), 107535.

Alghamdi, A. M. (2021). Fast and versatile pathway in fabrication of polyelectrolyte multilayer nanofiltration membrane with tunable properties. *Journal of Chemistry*, *2021*, 1-6.

Alghamdi, A., and Fadhillah, F. (2020). Thin film composite polyelectrolyte multilayer nanofiltration membrane fabricated using spin assisted layer by layer assembly: Application of solution diffusion film model. *Communications in Science and Technology*, *5*(1), 10-15.

Barro, L., Delila, L., Nebie, O., Wu, Y. W., Knutson, F., Watanabe, N., Takahara, M., and Burnouf, T. (2021). Removal of minute virus of mice-mock virus particles by nanofiltration of culture growth medium supplemented with 10% human platelet lysate. *Cytotherapy*, *23*(10), 902-907.

Chiarelli, P. A., Johal, M. S., Casson, J. L., Roberts, J. B., Robinson, J. M., and Wang, H. L. (2001). Controlled fabrication of polyelectrolyte multilayer thin films using spin-assembly. *Advanced Materials*, *13*(15), 1167-1171.

Cho, J., Char, K., Hong, J. D., and Lee, K. B. (2001). Fabrication of highly ordered multilayer films using a spin self-assembly method. *Advanced Materials*, *13*(14), 1076-1078.

Cho, K. L., Hill, A. J., Caruso, F., and Kentish, S. E. (2015). Chlorine resistant glutaraldehyde crosslinked polyelectrolyte multilayer membranes for desalination. *Advanced Materials*, *27*(17), 2791-2796.

Decher, G. (1996). Layered nanoarchitectures via directed assembly of anionic and cationic molecules. *Comprehensive Supramolecular Chemistry*, *9*, 507-528.

Decher, G., and Schmitt, J. (1992). Fine-tuning of the film thickness of ultrathin multilayer films composed of consecutively alternating layers of anionic and cationic polyelectrolytes. *Trends in Colloid and Interface Science VI*, *89, 160*-164

Dubas, S. T., and Schlenoff, J. B. (2001). Swelling and smoothing of polyelectrolyte multilayers by salt. *Langmuir*, *17*(25), 7725-7727.

Fadhillah, F., Alghamdi, A. M., Alsubei, M. D., and Aljlil, S. A. (2021). Synthesis of protein-fouling-resistance polyelectrolyte multilayered nanofiltration membranes through spin-assisted layer-by-layer assembly. *Journal of King Saud University-Engineering Sciences*, *33*(2), 81-87.

Fadhillah, F., Javaid Zaidi, S. M., Khan, Z., Khaled, M., and Hammond, P. T. (2011). Reverse osmosis desalination membrane formed from weak polyelectrolytes by spin assisted layer by layer technique. *Desalination and Water Treatment*, *34*(1-3), 44-49.

Gu, J. E., Lee, J. S., Park, S. H., Kim, I. T., Chan, E. P., Kwon, Y. N., and Lee, J. H. (2015). Tailoring interlayer structure of molecular layer-by-layer assembled polyamide membranes for high separation performance. *Applied Surface Science*, *356*, 659-667.

Hu, P., Yuan, B., Niu, Q. J., Chen, K., Xu, Z., Tian, B., and Zhang, X. (2022). Modification of polyamide nanofiltration membrane with ultra-high multivalent cations rejections and mono-/divalent cation selectivity. *Desalination*, *527*, 115553.

Jin, W., Toutianoush, A., and Tieke, B. (2003). Use of polyelectrolyte layer-by-layer assemblies as nanofiltration and reverse osmosis membranes. *Langmuir*, *19*(7), 2550-2553.

Kamp, J., Emonds, S., Seidenfaden, M., Papenheim, P., Kryschewski, M., Rubner, J., and Wessling, M. (2021). Tuning the excess charge and inverting the salt rejection hierarchy of polyelectrolyte multilayer membranes. *Journal of Membrane Science*, *639*, 119636.

Kim, K. S., Lee, K. H., Cho, K., and Park, C. E. (2002). Surface modification of polysulfone ultrafiltration membrane by oxygen plasma treatment. *Journal of Membrane Science*, *199*(1-2), 135-145.

Krasemann, L., and Tieke, B. (2000). Selective ion transport across self-assembled alternating multilayers of cationic and anionic polyelectrolytes. *Langmuir*, *16*(2), 287-290.

Lajimi, R. H., Abdallah, A. B., Ferjani, E., Roudesli, M. S., and Deratani, A. (2004). Change of the performance properties of nanofiltration cellulose acetate membranes by surface adsorption of polyelectrolyte multilayers. *Desalination*, *163*(1-3), 193-202.

Lau, W. J., and Ismail, A. F. (2009). Polymeric nanofiltration membranes for textile dye wastewater treatment: preparation, performance evaluation, transport modelling, and fouling control—a review. *Desalination*, *245*(1-3), 321-348.

Lee, K. P., Arnot, T. C., and Mattia, D. (2011). A review of reverse osmosis membrane materials for desalination—Development to date and future potential. *Journal of Membrane Science*, *370*(1-2), 1-22.

Li, P., Lan, H., Chen, K., Ma, X., Wei, B., Wang, M., Li, P., Hou, Y., and Niu, Q. J. (2022). Novel high-flux positively charged aliphatic polyamide nanofiltration membrane for selective removal of heavy metals. *Separation and Purification Technology*, *280*, 119949.

Liang, Y., and Lin, S. (2020). Mechanism of Permselectivity Enhancement in Polyelectrolyte-Dense Nanofiltration Membranes via Surfactant-Assembly Intercalation. *Environmental Science and Technology*, *55*(1), 738-748.

Oatley-Radcliffe, D. L., Walters, M., Ainscough, T. J., Williams, P. M., Mohammad, A. W., and Hilal, N. (2017). Nanofiltration membranes and processes: A review of research trends over the past decade. *Journal of Water Process Engineering*, *19*, 164-171.

Petersen, R. J. (1993). Composite reverse osmosis and nanofiltration membranes. *Journal of Membrane Science*, *83*(1), 81-150.

Qiao, K., Liu, H., and Hu, N. (2008). Layer-by-layer assembly of myoglobin and nonionic poly (ethylene glycol) through ion–dipole interaction: An electrochemical study. *Electrochimica Acta*, *53*(14), 4654-4662.

Rajabzadeh, S., Liu, C., Shi, L., and Wang, R. (2014). Preparation of low-pressure water softening hollow fiber membranes by polyelectrolyte deposition with two bilayers. *Desalination*, *344*, 64-70.

Razon, B. C. (2020). COVID-19: Impetus for “community spirits” among Filipinos. *Indonesian Journal of Science and Technology*, *5*(2), 26-33.

Richardson, J. J. (2015). Bj rnmalm m, caruso f. Technology-driven layer-by-layer assembly of nanofilms. *Science*, *348*(6233), 2491.

Ritcharoen, W., Supaphol, P., and Pavasant, P. (2008). Development of polyelectrolyte multilayer-coated electrospun cellulose acetate fiber mat as composite membranes. *European Polymer Journal*, *44*(12), 3963-3968.

Schlenoff, J. B., Dubas, S. T., and Farhat, T. (2000). Sprayed polyelectrolyte multilayers. *Langmuir*, *16*(26), 9968-9969.

Schmitt, J., Gruenewald, T., Decher, G., Pershan, P. S., Kjaer, K., and Loesche, M. (1993). Internal structure of layer-by-layer adsorbed polyelectrolyte films: a neutron and X-ray reflectivity study. *Macromolecules*, *26*(25), 7058-7063.

Shannon, M. A., Bohn, P. W., Elimelech, M., Georgiadis, J. G., Marinas, B. J., and Mayes, A. M. (2008). Science and technology for water purification in the coming decades. Nature, *452*(7185), 301–310.

Touir, J., Kitanou, S., Zait, M., Belhamidi, S., Belfaquir, M., Tahaikt, M., .Taky and Elmidaoui, A. (2021). The comparison of electrodialysis and nanofiltration in nitrate removal from groundwater. *Indonesian Journal of Science and Technology*, *6*(1), 17-30.

Wang, S., Xiao, K., Mo, Y., Yang, B., Vincent, T., Faur, C., and Guibal, E. (2020). Selenium (VI) and copper (II) adsorption using polyethyleneimine-based resins: Effect of glutaraldehyde crosslinking and storage condition. *Journal of Hazardous Materials*, *386*, 121637.

Wang, S., Yang, L., Wang, Q., Fan, Y., Shang, J., Qiu, S., and Wu, X. (2018). Supramolecular self-assembly of layer-by-layer graphene film driven by the synergism of π–π and hydrogen bonding interaction. *Journal of Photochemistry and Photobiology A: Chemistry*, *355*, 249-255.

Wu, C., Zhao, L., and Zhang, Y. (2017). pH-Responsive nanofiltration membranes based on porphyrin supramolecular self-assembly by layer-by-layer technique. *RSC Advances*, *7*(75), 47397-47406.

Yacouba, Z. A., Mendret, J., Lesage, G., Zaviska, F., and Brosillon, S. (2021). Removal of organic micropollutants from domestic wastewater: The effect of ozone-based advanced oxidation process on nanofiltration. *Journal of Water Process Engineering*, *39*, 101869.

Yoo, J. E., Lee, K. S., Garcia, A., Tarver, J., Gomez, E. D., Baldwin, K., Sun, Y., Meng, H., Nguyen, T. Q., and Loo, Y. L. (2010). Directly patternable, highly conducting polymers for broad applications in organic electronics. *Proceedings of the National Academy of Sciences*, *107*(13), 5712-5717.

Zhang, D., Lu, J., Shi, C., Zhang, K., Li, J., and Gao, L. (2021). Anti-corrosion performance of covalent layer-by-layer assembled films via click chemistry reaction on the copper surface. *Corrosion Science*, *178*, 109063.